



City Research Online

City, University of London Institutional Repository

Citation: Mudhar, R., Mucolli, A., Ford, J., Lira, C. & Yazdani Nezhad, H. (2022). Electrical and Magnetic Properties of 3D Printed Integrated Conductive Biodegradable Polymer Nanocomposites for Sustainable Electronics Development. *Journal of Composites Science*, 6(11), 345. doi: 10.3390/jcs6110345

This is the published version of the paper.

This version of the publication may differ from the final published version.

Permanent repository link: <https://openaccess.city.ac.uk/id/eprint/29152/>

Link to published version: <https://doi.org/10.3390/jcs6110345>

Copyright: City Research Online aims to make research outputs of City, University of London available to a wider audience. Copyright and Moral Rights remain with the author(s) and/or copyright holders. URLs from City Research Online may be freely distributed and linked to.

Reuse: Copies of full items can be used for personal research or study, educational, or not-for-profit purposes without prior permission or charge. Provided that the authors, title and full bibliographic details are credited, a hyperlink and/or URL is given for the original metadata page and the content is not changed in any way.

City Research Online:

<http://openaccess.city.ac.uk/>

publications@city.ac.uk



Article

Electrical and Magnetic Properties of 3D Printed Integrated Conductive Biodegradable Polymer Nanocomposites for Sustainable Electronics Development

Rajveer Mudhar ¹, Andiol Mucolli ¹, Jim Ford ², Cristian Lira ^{3,*}  and Hamed Yazdani Nezhad ^{1,*} 

¹ Advanced Composites Research Focused Group, Department of Engineering, School of Science and Technology, City, University of London, London EC1V 0HB, UK

² Department of Engineering, City, University of London, London EC1V 0HB, UK

³ Engineering Development, National Composites Centre, Bristol BS16 7FS, UK

* Correspondence: cristian.lira@nccuk.com (C.L.); hamed.yazdani@city.ac.uk (H.Y.N.)

Abstract: This article reports research on the development and implementation of new methods for structurally integrated and recyclable polymer based electronic products via multi-head fused deposition modelling (FDM) 3D printing. The focus of this research is to propose an efficient FDM-3D printing process utilising multiple filaments with no interruption of the process to ensure the multi-material electronic product achieved is structurally integrated. Such research is an attempt towards development of recyclable rigid electronic structures via multi-material 3D printing, i.e., multiple conductive nanomaterial embedded thermoplastic and non-conductive thermoplastic layers (in coil forms, herein). Six radio frequency identification (RFID) tag coil geometries were selected for the study. The thermoplastic polymer used in this research was polylactic acid (PLA), and the conductive filament was carbon black nanoparticle embedded PLA at approx. 21 wt.%. The nozzle and filaments diameters examined were 1.75 mm. A MakerBot Replicator 2X 3D printer was partially disassembled to be equipped with a dual head, for our examinations. The research investigated the major challenges ahead of the proposed development, mainly, on the deteriorating effects on the quality of the integrated product (structural integrity, electric and magnetic properties) induced by the 3D printing process parameters (e.g., temperature). The most efficient nozzle and bed temperatures to prevent visible defects were found to be higher than the supplier's recommendation, attributed to the uncertainties associated with the multi-material composition, and were found to require 248 and 100 °C for reliable and continued FDM printing, respectively. The measurements on the electric and magnetic properties, using 4-wire resistance and Hall effect method, respectively, were conducted to quantify process induced deteriorating effects, quantitatively. It has been examined whether the multi-material electronic structure can be achieved via uninterrupted (continuous) processing of polymer nanocomposite-based identification systems for recyclability purpose whilst maintaining the electromagnetic properties of it, a promising technology for reducing landfill. Recommendations were identified for best practices behind such development.

Keywords: 3D printing; nanocomposite; electrical conductivity; magnetic properties; carbon black; PLA; RFID



Citation: Mudhar, R.; Mucolli, A.; Ford, J.; Lira, C.; Yazdani Nezhad, H. Electrical and Magnetic Properties of 3D Printed Integrated Conductive Biodegradable Polymer Nanocomposites for Sustainable Electronics Development. *J. Compos. Sci.* **2022**, *6*, 345. <https://doi.org/10.3390/jcs6110345>

Academic Editor: Tien-Think Le

Received: 8 September 2022

Accepted: 2 November 2022

Published: 7 November 2022

Publisher's Note: MDPI stays neutral with regard to jurisdictional claims in published maps and institutional affiliations.



Copyright: © 2022 by the authors. Licensee MDPI, Basel, Switzerland. This article is an open access article distributed under the terms and conditions of the Creative Commons Attribution (CC BY) license (<https://creativecommons.org/licenses/by/4.0/>).

1. Introduction

Recycling was introduced, and increased drastically, after World War II ended in 1945 resulting in rationing and shortages of products. Moving forward, recycling has become more of an every-day activity that people take part in, however there is a lot of information missing from the understanding of recycling in general, and of multi-material systems specifically. This misinterpretation can result in more materials that have the potential to be recycled being sent to landfill or to be incinerated. Promoting the importance of recycling will lead to benefits for health, economy, and conservation of the planet.

In the UK, recyclable waste materials are collected as a combination of paper, mixed plastics, metal, and glass [1]. After collection, they are sorted using a materials recovery facility (MRF), which includes the process of emptying the recyclable waste onto a conveyor belt and encountering different methods of extraction and separation. Manual separation is required at the beginning to remove items that are not recyclable, possible hazards, or problematic materials. Firstly, flattened boxes are removed by the continuation of its movement along the conveyor while the other materials fall below, the metals (abundant in electronic devices) are extracted using a magnet, non-ferrous metals from non-metallic materials are separated by inducing Eddy Current leaving glass and plastics, e.g., Eddy Current Separators by Bunting Magnetics Ltd.

1.1. Polylactic Acid (PLA) Material and Its 3D Printing

The selection of plastics present is separated using optical sorting which uses infrared machinery. Polylactic acid (PLA) is a biodegradable material that is not recycled with the other plastics due to its lower melting point. PLA has a Resin Identification Code (RIC) 7 which belongs to Miscellaneous, with the inclusion of plastics that are not recycled [2]. PLA is also a bioplastic, and can be degraded using specific conditions and services, however if it is transported to landfill, it will behave like any other plastic, and not degrade [3].

The filament used for fused deposition modelling (FDM) based 3D printing [4] are commonly thermoplastics due to its ability to be melted and remoulded numerous times. The layers build on each other and material is deposited using the molten filament that has been extruded by the nozzle where its movements are controlled by a computer. For different materials, varying settings are required, and this can be adjusted with the use of a computer software that communicates directly with the printing machine.

As a common thermoplastic filament, PLA is labelled as a bioplastic that has been derived from plant-based materials such as corn and fermented starch. PLA can also be made through condensation of lactic acid. Because of its organic and natural foundation, PLA is suitable for products that come into contact with food and its packaging such as beverage cups [5], and also in the biomedical industry including, devices to enhance bone fixations and surgical suturing. To further support the use of PLA in the medical industry, research has been conducted by Vaňková in 2020 [6] on the implementation of 3D printed masks to help stop the spread of Coronavirus Disease 19 (COVID-19). This would work by creating the mask especially for more than one use, thus it would need to endure frequent cleaning and sanitisation.

PLA can be recycled, but only if it is not contaminated with other materials, or plastics. Within the current recycling systems, it is quite difficult to classify and group from other polymers, and for this reason if they are not separated it is sent to landfill. When PLA is sent to recycling it is usually in the form of leftover pieces of filament from 3D printing, where a specific recycling facility can grind it into powder to extrude the material again into filament for 3D printing after mixing several batches sourced from multiple leftover PLA material.

It should be noted that although PLA is regarded as a bioplastic which has been produced using renewable resources, it is not naturally possible to achieve the conditions in which it can biodegrade. A study demonstrated by Kjeldsen et al. [7] at the Industrial Biotechnology Innovation Centre, shows that PLA can biodegrade. The study tested different types of environments, conditions with varying bioplastics, and recording the biodegradability over a period of days. The environments of the study were mostly either compost or soil, and the conditions for biodegradation varied in temperature and humidity. From these results it can be seen that in any of the given conditions and environments, PLA can degrade, of a range starting from 10 to 100% from the number of days ranging from 28 to 98. The conditions for a higher percentage of biodegrading appear through temperatures of 58 °C, in synthetic materials, and in high moisture. These conditions are

not guaranteed every day, and not in all parts of the world, which further proves that the biodegrading of PLA can only be ensured in specific conditions [7].

Other than biodegrading, there are other methods of repurposing PLA via a group of materials that were specifically only PLA, there are two methods of recycling, chemical and mechanical. The chemical recycling of PLA was studied by McKeown et al. in 2020 [8], and the research shows that the process should be more cost efficient than other modes of transforming PLA. The methods of mechanical recycling of PLA were analysed by Beltrán et al. in 2021 [9] where the PLA was washed and melted by extrusion. This was then transformed into film by compression moulding. Through this research, the films under biodegrading testing were disintegrated within 21 days presenting the idea of the biodegradation of the material. The other films were analysed and showed crystallising appearing on the film. It was also mentioned that there was a significant effect on the physical properties of the material, which would be a disadvantage for the products that require a specific aesthetic.

1.2. Radio Frequency Identification (RFID)

A way to decrease the mix up of materials is to add an identification system on the materials to reduce the human error of sending materials to the wrong location. The ID system used in this study is radio-frequency identification which is not unlike barcoding as it stores information. Radio frequency identification (RFID) works on the idea that information can be stored on a material passively with the use of electrical circuits [10] Passive tags must be charged before being independently used, and active tags require an internal energy source.

RFID works with the use of radio waves by identifying, storing, and presenting data (in computer systems). Its tags consist of an integrated circuit and these systems work using the tag, RFID reader, antenna, and a chip. The tags are easy to use and require little human intervention on the information sharing process, but on the other hand they are time consuming to set up and require more advanced technology in order to be used successfully.

As RFID systems are a more recent technology compared to other ID systems such as barcodes, it has not been developed to its utmost ability. The RFID tag technology has to date focused on efficient functionality, and so properties such as its recyclability were the most important factor explored to date. The main component of an RFID tag is the antenna, it receives and transmits information to and from the RFID reader and the chip. It is usually made from thin metallic strips of aluminium, copper, or silver due to their high conductivity, malleability, and melting point. The antenna can have different geometries with a varying number of coils.

An automatic identification and data capture system (AIDC) is the term used to describe the process of gathering and collecting information that is entered into a computer system—without the need of human interference. AIDC systems include barcodes, RFID, and biometric systems, for example using voice or iris recognition for unlocking a smartphone. Barcodes can exist as either 1-dimensional (1D) or 2-dimensional (2D), which is also known as a Quick Response (QR) code. Both of these are used frequently, for different reasons. These barcodes are usually used in retail store operations to scan an item through the buying process, or in warehouses in order to check stock and inventory. The QR codes are used for accessing websites and for authentication when signing into an account [11]. Both codes are useful and often used, however they are susceptible to physical damage, including weathering, scratches and anything that may obstruct the image of the barcode, which make retrieving the information impractical.

A few ways to enhance the barcode identification system can be through collaborating with visual labelling, for example the process of film-insert moulding (FIM). This enables the label to be graphically moulded onto the material creating a graphical image that cannot be removed. According to an article published by ScreenPrinting, this type of identification was also beneficial as it would allow for magnetic inks, incorporating circuitry and compressing semiconductor chips; however, on the other hand with adding more

colours and graphics onto PLA, if completed incorrectly, it can result in a more toxic product when being used and recycled, as stated by an article published on *Plastics Decorating*. With the integration of magnetic inks there could be a possibility of using FIM to create an embedded RFID.

An RFID tag can have numerous shapes and sizes, and can have different forms, for example, an embeddable RFID coil. It has the most technological advantages as it is a newer form of identification. RFID is also advantageous as it already shows some use when in warehousing operations that are more efficient than barcodes, due to the long-read range and the ability for the tag to be read at any orientation. RFID systems usually appear in the form of an adhesive that can be attached to a variety of materials, for example when security tagging specific items in a retail store, however research conducted by Leung et al. (2007) [12] studied the behaviour of a polymer-based antenna on curved surfaces. It showed that the performance and the distance at which the RFID reader can receive data decreased as the surface of the material grew in curvature. Knowing this, the dimensions of the antenna created for this project had to be considered, a relatively large antenna would have a risk of experiencing more curvature than a smaller one. Such research has been completed by different companies to try and find an alternative to create sustainable RFID technology. The company Storaenso in 2020 had created an ‘eco-RFID tag’ without the use of plastic. It is comprised of an adhesive made from renewable paper and magnetic ink to create the printed RFID label. Although it has eco-friendly potential, the adhesive polymer cannot guarantee adhesion to the material, nor the ease of removal before it goes through the recycling process [13].

The reason that RFID is not used in the process of identifying and separating plastics is due to the material composition of the tag. The main component of the operation is the antenna which is usually made from copper, silver, or aluminium. These materials are chosen because of their conductivity as well as flexibility. The adhesive RFID on a plastic product would not be recycled as they are composed of dissimilar materials and would be sent to landfill. Therefore, the components that make up the current RFID adhesive tags may cause issues in efficiency of recycling processes [14].

1.3. The State of the Current Research

The current research considers the FDM 3D printing process of recyclable polymer-based RFIDs, specifically PLA, and aims to develop an approach to make PLA recycling more efficient, to ensure PLA has a longer product lifetime, and to reduce the number of items that are sent to landfill as an ultimate aim. Recycling is a procedure that occurs every day, it has its benefits, but drawbacks too. For example, if distinct groups of materials are not separated appropriately, it can cause an unnecessary number of products to end up in landfill—resulting in damaging effects on the environment and in turn, human health. For this project, an identification (ID) system was used to enhance the classification element of the recycling process. The main component is the antenna, and it is usually made from materials that are not compatible to be recycled with PLA. Using a conductive PLA based multi-material, a 3D printed ID system antennae was produced for the purpose of this study.

The RFID model was developed using SolidWorks to model the product, and utilised a MakerBot Replicator 2X to 3D print. From this print, a material characterisation phase of conductivity and magnetic constant measurements was conducted before and after the printing, and the effects of the printing process on such properties were investigated.

Most of the research was completed on identification methods and plastic materials, such as RFID tags and PLA. These two components were chosen for the current research. The main objective of this study was to primarily develop a straightforward and uninterrupted (continuous) multiple filament FDM process for recyclable tags. The final product was comprised of dual material flat RFID coils as a demonstration of how the main body of a conductive PLA nanocomposite based identification system can be directly printed onto plastic material. PLA is not recycled with the other types of plastic since it is in the

miscellaneous category. Therefore, to enable a highly efficient recyclable multi-material structure, it is desirable to fabricate the entire structure from the PLA based filaments. Even though it is a compostable plastic, it usually ends up in landfill where it does not break down.

The recycling process is made up of a few phases to make recycling efficient, however these processes are correct to any specific material group. One of the main issues of recycling is the number of products that go to landfill due to the lack of or incorrect allocation of materials. Ensuring an identification system for PLA can identify, classify, and reduce the number of materials sent to landfill. Therefore, the focus of the current research was to assess the initial step for a PLA based identification system that could be integrated in multiple layers/materials without process interruption while maintaining the electromagnetic properties. The effect of difference in RFID tag geometries on the properties was also investigated.

2. Experimental Approach

The implementation of identification systems could be escalated to other polymers and possibly other material groups. After discovering the way in which PLA is recycled, to aid the study's aforementioned objective was to determine what phase during the recycling process could be enhanced and the reasoning for that. Firstly, the broader actions to recycling were named as collection, cleaning, sorting, reprocessing, and finally the re-use of products. This created a looped system that would extend a materials product lifetime. After this, each step was broken down into its components, for example, advancements could be made through the collection of materials by changing how the users separate their materials, or through sorters whereby the method for sorting materials is more manual than mechanical. The process under consideration is the sorting process, as the advancements made in this phase do not disturb or disrupt the users or workers usual routine to an extreme scale. A point of the sorting phase, the improvement made was the ability to sort through RIC 7 to be able to gather the same materials and reduce the number of different types of products in this category. The identification system aimed to be a physically discreet method of finding a certain material—in this case PLA—and grouping them together.

When using identification systems, it is important to take into consideration the properties of each of them. For this project RFID technology was used over barcodes due to its ease of accessing data from a distance, ability to rewrite data on the tag, and unlike barcodes, RFID technology tags have a lower chance of being damaged such as, due to weathering, or proximity to chemicals. Furthermore, multiple RFID systems can be read at a time at a longer distance with any orientation, whereas barcodes are required to be facing the scanner at a shorter distance [15]. Another advantage of the use of RFID technology is that the reading and collection of data does not require human involvement after the system has been established, reducing the human error whilst retrieving data. As such, the properties of different RFID coil antenna geometries were investigated post the 3D printing process.

A filament of conductive PLA was 3D printed to be used to imitate the conductive component of the antenna. The antenna was printed onto a plate of regular PLA, and durability of the final product was studied. The antenna made from a conductive polymer embedded with carbon black nanoparticles printed onto a flat surface acted as an integrated antenna and identification system on the material that was not required to be removed before recycling—an advantage of the proposed integrated multi-material solution.

Lastly, in order to complete the assessments, the method of welding the two materials together was completed by using a MakerBot Replicator 2X 3D printer. The machine was partially disassembled and equipped with a dual head to allow simultaneously feeding of two separate filaments (non-conductive and conductive PLA filaments), to ensure there is no interruption of the 3D printing process.

The model used for printing consisted of four different geometries of coils with a different number of rotations, 5 and 10, covering identical areas over a base plate, with dimensions 10 cm × 20 cm. The coils were labelled as Round (R), Square (S) and Hexagon (H). Five rotation coils were labelled '1' with thicker width, with 10 rotation ones labelled '2' with thinner width. These coils were made from conductive PLA filament, whilst the base that it was attached on was made from ordinary PLA filament. The design shown in Figure 1 was created and assembled using a commercial CAD software, SolidWorks.

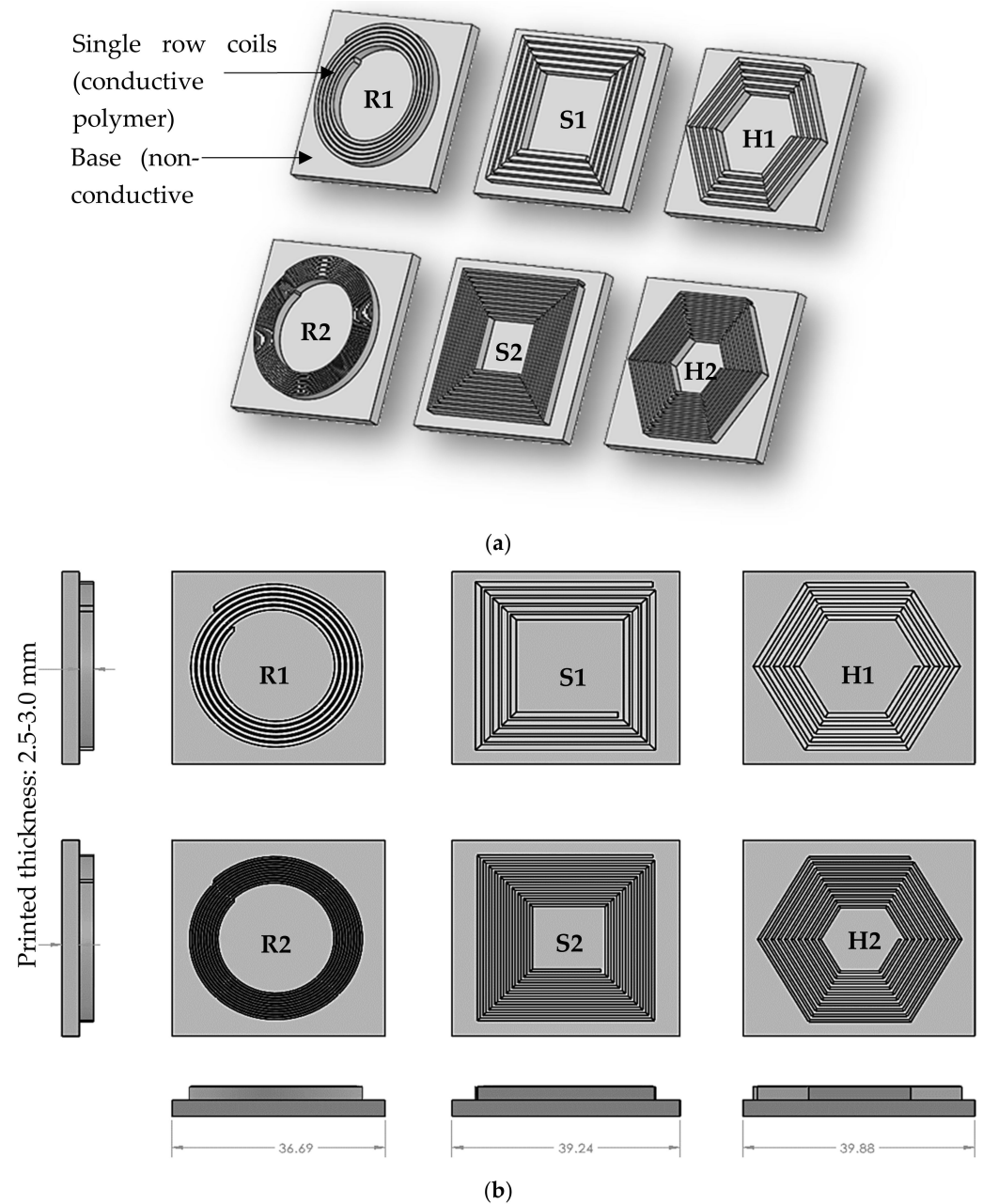


Figure 1. CAD model of the round, square and hexagon coils with thick (1) and thin (2) widths developed for 3D printing in (a): 3D and (b): top views; R: Round coil, S: Square coil, H: Hexagon coil.

Optical microscopy was conducted post printing for the identification of the gaps developed due to the inherent 3D printing precision, between the materials. Such observations were necessary to identify the proper printing parameters for a reliable and continued production. It was found that such parameters required for our multi-material printing exceeds the ones specified in the supplier’s data (discussed below). In addition to this, the

effects of 3D printing on the material's electrical conductivity and magnetism were then analysed by measuring the resistance of the filament using 4-wire technique before and after printing, described in Section 4.

3. Materials and Manufacturing

The material under examination in the research was a 21 wt.% conductive carbon black particle embedded PLA which had been manufactured by Proto-Pasta in the format of 1.75 mm-diameter filaments (AMOLEN filament product CDP1170 supplied by Proto-Pasta). It is a composite that is formed of 4043D PLA [16]. Carbon black is commonly used in a range of products, e.g., utilised in automotive components as a reinforcing agent due to its strengthening properties. Its structure is similar to graphite where it is formed of sheets of carbon atoms.

For this project, the print settings varied in order to achieve a print that presented a minimal number of defects according to the optical microscopic observations. The first iteration of platform and nozzle temperatures were 60 °C and 215 °C, respectively, as these were suggested by the manufacturer. The settings that enabled an efficient print of conductive PLA (i.e., with no or slight defects) that enabled an uninterrupted printing were a bed temperature of 100 °C and a nozzle temperature of 248 °C.

There were challenges at the trial level with the recommended printing parameters. During the printing process the melted filament laying process occasionally experienced disbond defects between layers which was resolved with higher temperature adjustment. Figures 2 and 3 show the defects that occurred when printing a test piece of conductive PLA. The major driver for this problem was identified as the recommended temperature specified in the filament's supplier specification, which was found lower than required for sufficient softening/melting of the filament. As a direct consequence the extruder motor was not powerful enough to retrieve the filament and move it through the nozzle for successful printing. This challenge has been overcome via speed, and setting a higher temperature.

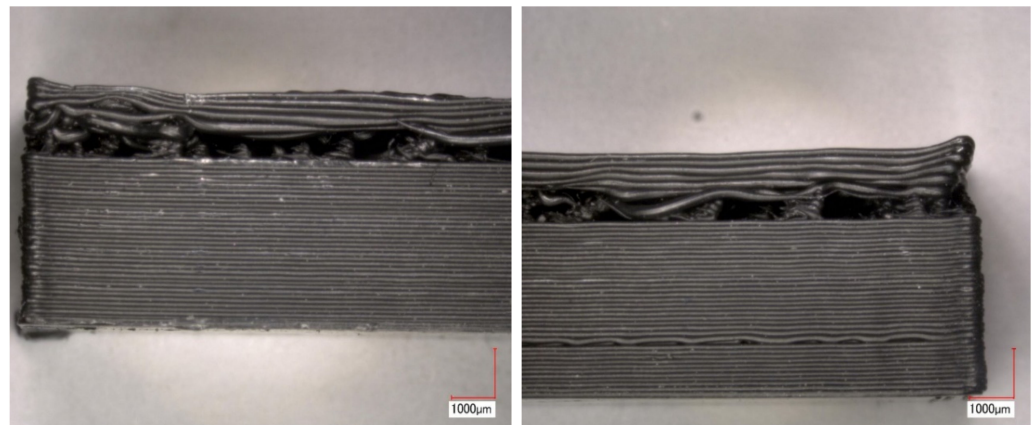


Figure 2. Defects occurring in test prints.

The extruding temperature on print settings proposed for normal PLA filament on the MakerBot software is 215 °C.

The suggested temperature of was updated to an higher value: 248 °C. Such variation in nozzle extruder temperature was due to the heat dissipated from the platform bed, and also due to the difference in machines used. With the aim to solve the printing challenge, the settings were experimented over a range of temperatures between 215 and 248 °C to identify the best extruder temperature for a macroscopically defect free printed part.

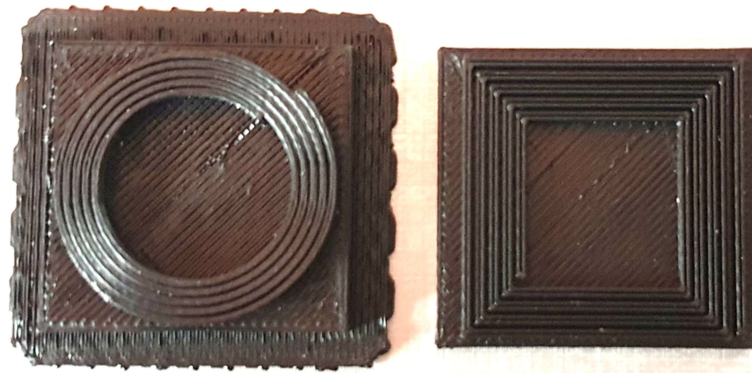


Figure 3. Defects occurring on the base polymer despite successful coils printing.

The success of dual head printing with conductive and non-conductive filaments can be used in the future for RFID tagging on PLA materials as the conductive PLA coil acted as the largest component of the tag in place of copper, aluminium, or silver.

It was examined that for the relatively longer printing duration, the printed base plate could not retain as much heat from the printing process as the main process variable for binding the two materials was the temperature [17].

4. Results and Discussion

After testing the 3D printing process by printing trial models, the next step was to print the product using the dual head nozzle of the printer. The base was constructed of normal PLA filament, and the coils were made of conductive PLA. 2–3 samples per coil category were printed to ensure the repeatability of the customised process and measurements. Typical printed RFID structures are shown in Figure 4.

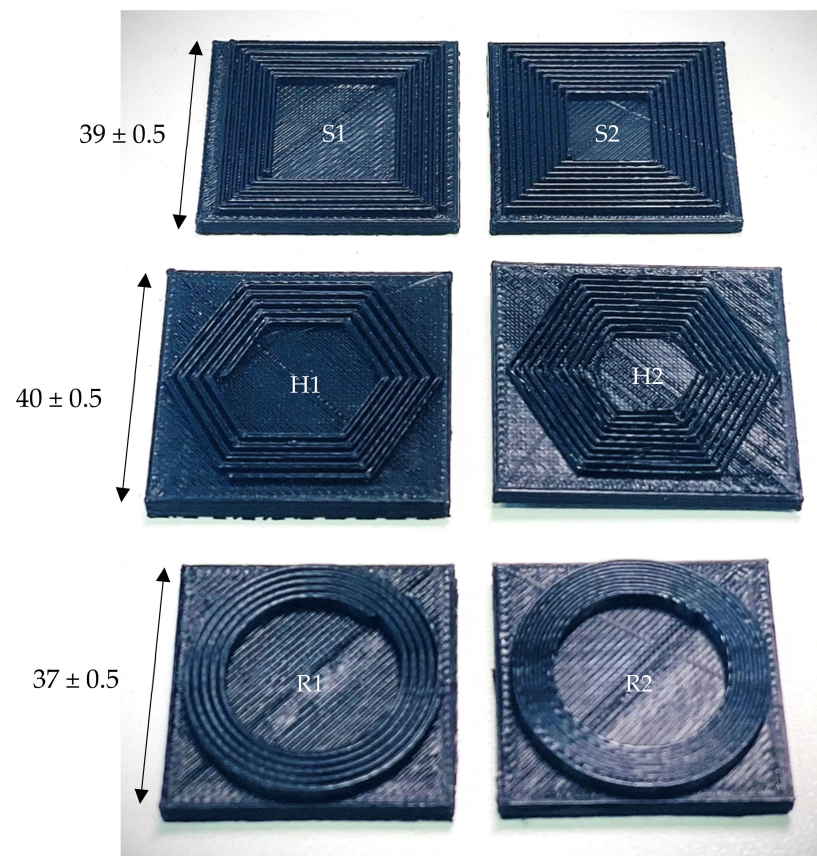


Figure 4. Typical trimmed-off 3D printed products.

Two methods were used to test material properties before and after the 3D printing process, firstly by assessing the conductivity and magnetic properties of the material, and secondly using optical microscopy to identify and quantify the quality of the printed patterns.

4.1. Electrical Conductivity Measurements

Initially, in order to calculate the conductivity of the material, the resistance is measured along with the dimensions of the piece under testing. For retrieving this data, an ohmmeter was connected to both ends of the coils, and resistance was recorded after every five seconds using 2-wire method. However, significant fluctuations in the resistance values was observed due to the fact that lead wires may become in contact with either carbon black particles or polymer from time to time, with relatively low-value resistance. To overcome such issue, a 4-wire method was utilised:

Kelvin or 4-wire resistance measurement method consists of determining the resistance from Ohm's law ($R = V/I$) by using an AM-meter, voltmeter and four wires. In this method, two wires are used to deliver the current to the measuring piece and the other two wires to measure the voltage drop alongside the piece. A fixed current generator is used to provide a constant current through circuit. 4-wire method was then utilised for higher precision measurements in case of low-value resistance as it eliminates the effect of lead wires and the contact resistances. A typical setup for 4-wire measurement of the filament examined in our research is shown in Figure 5.

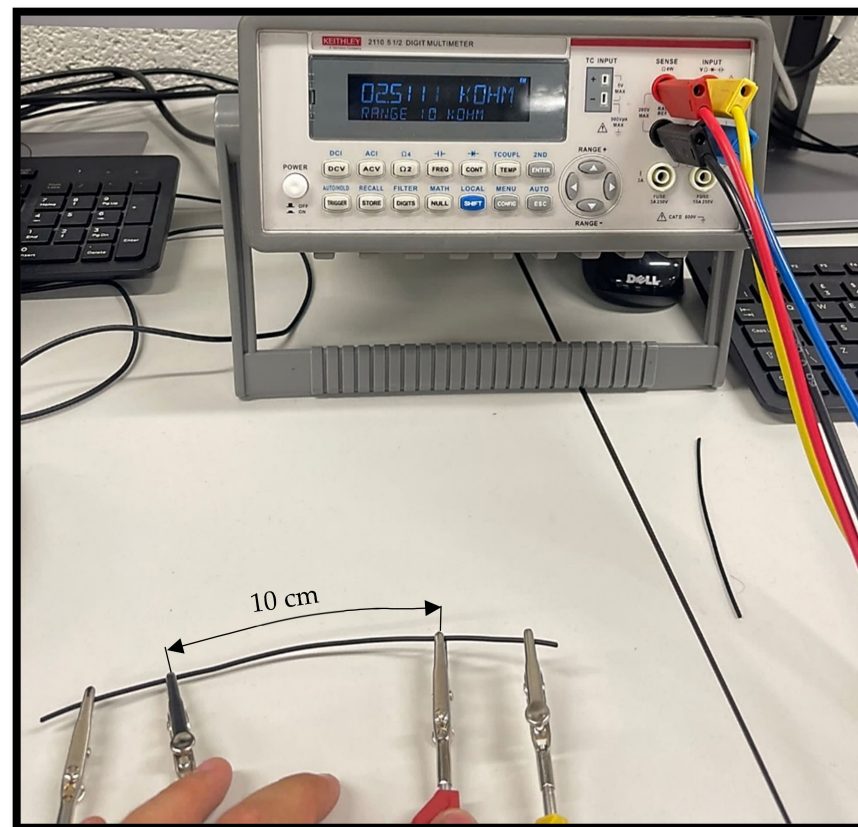


Figure 5. Typical 4-wire setup for filament's electrical resistance measurements conducted on filaments and coils.

The simplified linear formula for calculating conductivity in Siemens per metre length was then utilised for the comparative analysis of the samples, where $\sigma = L/RA$ ($= 1/\rho$), with σ , L , R , and A values corresponding, respectively, to the conductivity (S/m), coil length (m), resistance (Ω), and cross-sectional area (m^2), respectively, and ρ is the resistivity in $\Omega.m$.

Table 1 presents the average values of electrical resistance and conductivity of the different coil shapes printed. As seen, the measurements were taken in millimetres (mm) and kilo-ohms (kΩ), and these multipliers cancelled out to give the conductivity units of Siemens per metre (S/m). The results generally show that the resistivity of the RFID structures, post printing, is significantly reduced compared to the values measured from the pristine filament prior to printing, and thus the conductivity increases significantly. The detailed observations are as follows:

1. The conductivity clearly increases post printing, significantly, in all coils, when compared to the filament’s conductivity (meaning that the resistance decreases in all) by the order of six times in the case of R1 coil, and 150 times in the case of H2 despite the scattered data, i.e., increasing trend in all coils. This is attribute to the well-known phenomenon that 1- the printing process tends to align carbon black particles, and 2- shrinking the cooling polymer surrounding the particles occur post printing. The shrinking of the polymer post printing (apart from the induced polymerisation) is due to the significant mismatch in its coefficient of thermal expansion between the polymer and particles, meaning that the particles do not contract as much as the polymer does. Therefore, the contact between the conductive particles may be further established in a rigid medium (in contrast with a softer filament medium with loose and flexible particles contact) as identified with other carbon conductive mediums such as carbon nanotubes embedded polymers [18]. The two effects should add up to the significant increase in the conductivity.
2. Further investigation indicates that in all coils, the conductivity in thin coils with 10 rotations is greater than that in the thick ones with five rotations, attributed to relatively higher alignment of the conductive particles (discussed later). It is at minimum twice in square coils, and maximum six times in the other coils.

Table 1. Electrical conductivity and resistance data measured of test pieces (filament and printed).

Shape	Filament (*: Supplier Data)	Filament (This Research)	Round Coil		Square Coil		Hexagon Coil	
			R1	R2	S1	S2	H1	H2
Length [mm]	100 *	100	390	790	532	881	378	560
Sectional area [mm ²]	2.4	2.4	2.5	1.25	2.5	1.25	2.175	1.075
Resistance R [kΩ]	2–3 *	2.5–2.5	1.2–1.4	0.8–1.0	0.6–0.9	1.2–1.5	0.2–0.4	0.2–0.3
Resistivity ρ [kΩ.m]	4.81–7.22 (×10 ⁻⁵)	6.04–6.06 (×10 ⁻⁵)	7.7–9.0 (×10 ⁻⁶)	1.3–1.6 (×10 ⁻⁶)	2.8–4.2 (×10 ⁻⁶)	1.7–2.1 (×10 ⁻⁶)	1.1–2.3 (×10 ⁻⁶)	3.8–5.8 (×10 ⁻⁷)
Conductivity σ [S/m]	13.9–20.8	16.5–16.6	111.4–130.0	632.0–790.0	236.4–354.7	469.9–587.3	434.5–869.0	1736.4–2604.7

R: round coils, S: square coils, H: hexagon coils, 1: thick coils, 2: thin coils.

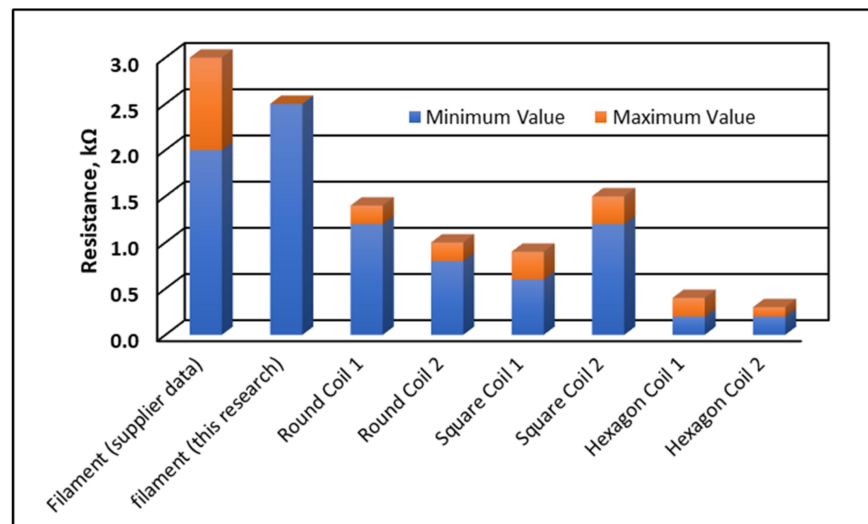
It is noteworthy that non-conductive-doped polymer should be a dielectric—ideally good insulator, and it makes it difficult to measure any resistance but infinity in an ideal insulator such as dielectric particle or polymer, e.g., [19]. At the phenomenological actual scenario, this may be described as follows:

- The resistance of the conductive doped 3D printed material (i.e., conductive particles bonded in a polymer lattice) varies significantly with temperature induced effects throughout the 3D printing. As evidence, this effect has been commercialised to make sharp knee positive temperature coefficient thermistors for resettable (self-reset) circuit protection, such as “Multifuse” or “Polyswitch” [20].
- These devices have low resistance at room temperature, but when they are self-heated (above a switching point) by excess or heavy current flowing through, the now-warmed polymer softens its grip on those conductive particles (establishing loose contacts), and the device switches to a high resistance state with just enough current to stay hot until the reset point by a manual disconnection. This can occur repeatedly with little aging; i.e., some such devices can switch quite high currents (e.g., in automotive electrical protection) and others can safely switch mains supply voltages such as 230 V AC, and are used to protect electromagnetic appliances such as transformers, motors, etc, and electronics.

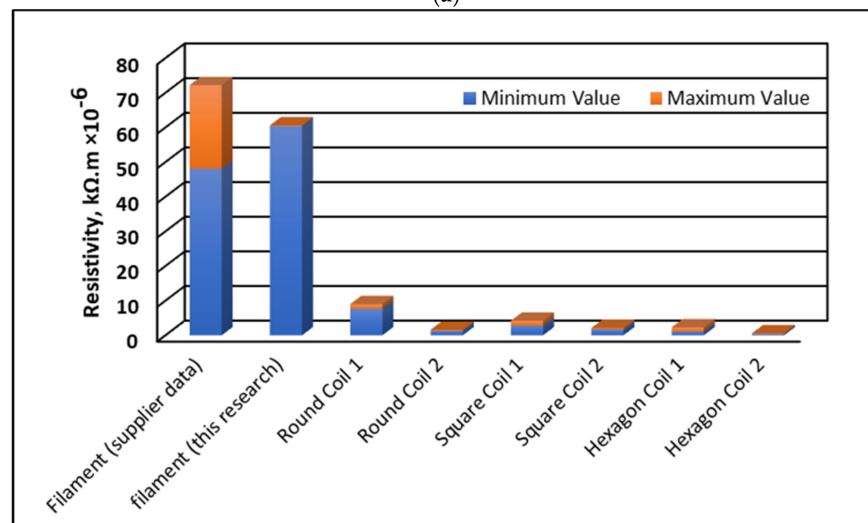
The 4-wire method utilised in the current research should eliminate the probe/contact resistances described above, in an approach that:

1. If either/both the drive circuit probe/s has too high impedance to pass the test current, the instrument should error.
2. The measuring circuit has very high (10 Gohm) internal impedance, so unless its probes are almost insulated there is very little error in such measurement (due to the miniscule current drawn by the instrument as a millivolt meter) either.

The data variations are presented in Figure 6a–c, respectively, for electrical resistance, resistivity and conductivity. As seen, the resistance and consequently resistivity decreases post 3D printing in all samples post printing when compared to that of the filaments. Equivalently, the conductivity increases significantly in all categories, with the highest increase observed in R2, S2, H1 and H2. It is observed that the thin samples (indexed as '2') of all categories achieve a higher conductivity, owing to its thinner coil configuration and attributed to a relatively denser conductive filament alignment. Expectedly, the resistivity follows the variation of the ratio of A/L , calculated from the resistance values (Figure 7).

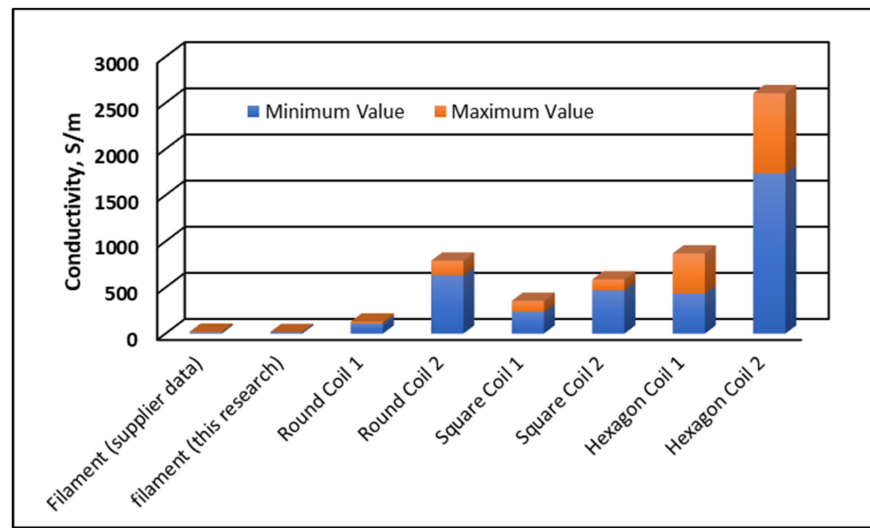


(a)



(b)

Figure 6. Cont.



(c)

Figure 6. Evolution of electrical properties with coils type and dimensions; (a) electrical resistance R , (b) resistivity ρ , and (c) conductivity σ .

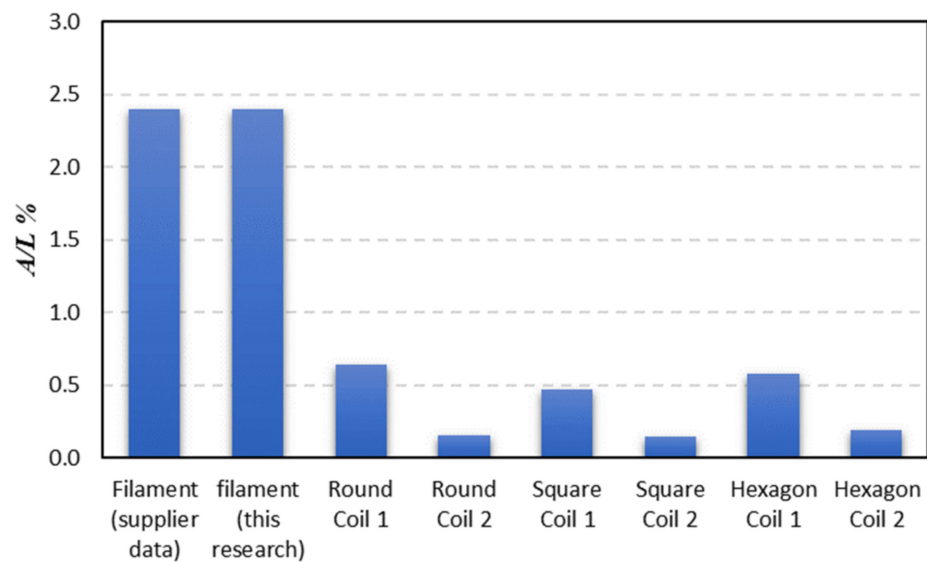


Figure 7. Variation of A/L percentage in filaments and coils.

Despite the significant enhancement in the electrical conductivity values post printing, its disparity between the coils is described as a function of A/L . The authors believe that an elaborative description for such disparity would require further investigations using real-time process and electrical measurements during the printing of the coils. Moreover, a few microscopic investigations presented possible bonding between coil’s patterns during printing that could increase the effective electrical area, and thus deteriorate the conductivity via increasing the resistivity. Figure 8 presents typical microscopic images of R2 coil where such bonding was observed.

4.2. Magnetic Measurements

The magnetic strength of the samples prior to and post 3D printing was also measured using an Extech gaussmeter SDL900 utilising the Hall effect in which a magnetic field in the transverse and perpendicular direction to an induced electric current is measured (Figure 9). Multiple locations in each sample were measured to ensure repeatability of the data, and to work out the data scatter. The samples were allowed to cool down at room temperature post printing, to ensure no temperature induced magnetic decay. The filaments exhibited

0.04–0.08 milli-Tesla (mT) strength owing to its carbon black particles (neglecting the PLA's relatively lower magnetic properties) while the coils post printing exhibited a significant reduction in that magnetic strength at 0.01–0.02 mT, approximately four times reduction after printing in all samples, as examined in multiple locations.

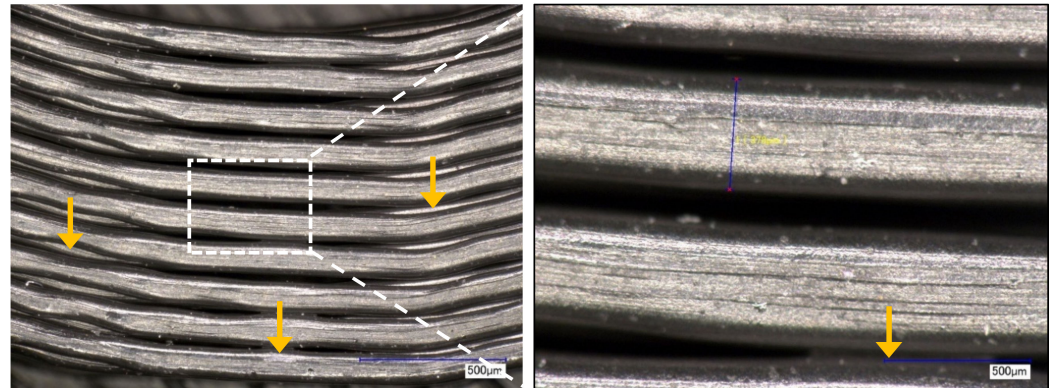


Figure 8. Typical microscopic images of R2 coils at 200× and 50× magnifications, representing bonding and contact between different 3D printed patterns distributed at different scales (shown by arrows).

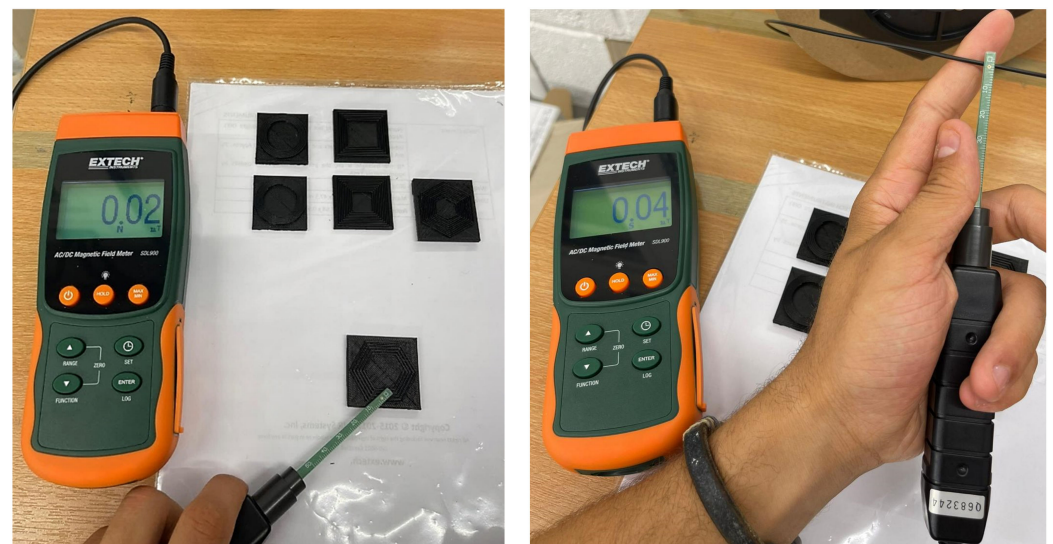


Figure 9. Magnetic strength measurement on the conductive filament (prior to the printing) and RFID coils (post printing).

The magnetic measurements were conducted following the Hall effect method in which a transverse voltage is initially measured in the Hall probe from which the magnetic force and thus the magnetic strength is quantified. Since, the probe measures a particulate magnetic medium (and not a homogenous materials with a continuum magnetic medium), in a high resistance medium a low electromotive force is induced (e.g., in the filament with low conductivity). Consequently, the voltage induced increases resulting from the polarity induced by positive charge carriers. The increase in the voltage results in the increase in the magnetic strength in the filament with relatively higher resistance. Such an effect is reversed in the printed coils, leading to a lower magnetic strength.

5. Conclusions

It was observed that the integration of the two materials differing in conducive properties was successful, with the conductivity of the final piece increased dramatically, a positive factor for suggesting a promising polymer based, rigid electronic structure printing.

This was enabled by a continuous uninterrupted, dual-header FDM 3D printing of PLA based nanocomposites embedded by 21 wt.% carbon black particles. However, it was observed that the magnetic strength was reduced by the order of four times compared to that of the filament.

The conductivity increase was attributed to the positive coupled effect of conductive particles curvilinear alignment in the shape of narrow coils and polymer shrinkage/bonding surrounding the carbon black particles enabling relatively higher particles contact. Instead, the magnetic strength driven by the polarity resulted from the positive charge carriers induced by the Hall effect measurement measurement, has demonstrated a behaviour proportional to the electrical resistance, i.e., higher magnetic strength in filaments and lower in printed coils. Despite such observations at the phenomenological level, further investigation would be required at microscale using real-time polarity and electrical measurements in situ with 3D printing and/or post printing, to identify and quantify the underlying micro-mechanisms underpinning such phenomenological behaviour of the 3D printed conductive PLA nanocomposites at macroscale.

Author Contributions: Conceptualization and supervision were made by H.Y.N. and C.L.; methodology, H.Y.N. and R.M.; formal analysis and investigation, R.M. and A.M.; electrical and magnetic measurements, J.F. and A.M.; writing—original draft preparation, R.M.; writing—review and editing, A.M. and H.Y.N.; All authors have read and agreed to the published version of the manuscript.

Funding: This research was funded by the UK Engineering & Physical Sciences Research Council (EPSRC), Ref. EP/R016828/1 (Self-tuning Fibre-Reinforced Polymer Adaptive Nanocomposite, STRAINcomp) and EP/R513027/1 (Study of Microstructure of Dielectric Polymer Nanocomposites subjected to Electromagnetic Field for Development of Self-toughening Lightweight Composites).

Institutional Review Board Statement: Not applicable.

Informed Consent Statement: Not applicable.

Data Availability Statement: The underpinning data can be accessed at <https://doi.org/10.25383/city.21370173> (accessed on 1 November 2022).

Acknowledgments: The authors are grateful to the technical supports from Keith Pamment and Richard Leach at the School of Science and Technology at City, University of London for the experimental research. The authors would like to acknowledge the grants received for this research from the UK Engineering & Physical Sciences Research Council (EPSRC), Ref. EP/R016828/1 (Self-tuning Fibre-Reinforced Polymer Adaptive Nanocomposite, STRAINcomp) and EP/R513027/1 (Study of Microstructure of Dielectric Polymer Nanocomposites subjected to Electromagnetic Field for Development of Self-toughening Lightweight Composites). The underpinning data can be accessed at <https://doi.org/10.25383/city.21370173> (accessed on 1 November 2022).

Conflicts of Interest: The authors declare no conflict of interest.

References

1. Environment Agency. *Guidance on Separate Collection of Waste Paper, Plastic, Metal or Glass*; Environment Agency: Bristol, UK, 2020.
2. McGill Environmental Systems of NC, Inc. *Grappling with the Infamous #7 PLA Recycling Code*; McGill Environmental Systems: New Hill, NC, USA, 2022.
3. Jiménez, L.; Mena, M.J.; Prendiz, J.; Salas, L.; Vega-Baudrit, J. Polylactic Acid (PLA) as a Bioplastic and its Possible Applications in the Food Industry. *J. Food Sci. Nut.* **2019**, *5*, 2–6.
4. Daminabo, S.C.; Goel, S.; Grammatikos, S.A.; Nezhad, H.Y.; Thakur, V.K. Fused deposition modeling-based additive manufacturing (3D printing): Techniques for polymer material systems. *Mater. Today Chem.* **2020**, *16*, 100248. [[CrossRef](#)]
5. Singhvi, M.; Gokhale, D. Biomass to biodegradable polymer (PLA). *RSC Adv.* **2013**, *3*, 13558–13568. [[CrossRef](#)]
6. Vaňková, E.; Kašparová, P.; Khun, J.; Machková, A.; Julák, J.; Sláma, M.; Hodek, J.; Ulrychová, L.; Weber, J.; Obrová, K.; et al. Polylactic acid as a suitable material for 3D printing of protective masks in times of COVID-19 pandemic. *PeerJ* **2020**, *8*, e10259. [[CrossRef](#)] [[PubMed](#)]
7. Kjeldsen, A.; Price, M.; Lilley, C.; Guzniczak, E.; Archer, I. A Review of Standards for Biodegradable Plastics. *Ind. Biotechnol. Innov. Cent.* **2018**, *33*, 33.
8. McKeown, P.; Jones, M.D. The Chemical Recycling of PLA: A Review. *Sustain. Chem.* **2020**, *1*, 1–22. [[CrossRef](#)]

9. Beltrán, F.R.; Arrieta, M.P.; Moreno, E.; Gaspar, G.; Muneta, L.M.; Carrasco-Gallego, R.; Yáñez, S.; Hidalgo-Carvajal, D.; de la Orden, M.U.; Martínez Urreaga, J. Evaluation of the Technical Viability of Distributed Mechanical Recycling of PLA 3D Printing Wastes. *Polymers* **2021**, *13*, 1247. [[CrossRef](#)] [[PubMed](#)]
10. Want, R. RFID: A key to automating everything. *Sci. Am.* **2004**, *290*, 56–65. [[CrossRef](#)] [[PubMed](#)]
11. Neagu, C. What Is a QR Code? *What Are QR Codes Used For? Digital Citizen*. 2021. Available online: <https://www.digitalcitizen.life/simple-questions-what-are-qr-codes-and-why-are-they-useful/> (accessed on 1 November 2022).
12. Leung, S.Y.Y.; Lam, D.C.C. Performance of Printed Polymer-Based RFID Antenna on Curvilinear Surface. *IEEE Trans. Electron. Packag. Manuf.* **2007**, *30*, 200–205. [[CrossRef](#)]
13. Storaenso. ECO RFID Explained—A Look Behind the World’s Greenest Tag. 2020. Available online: <https://www.storaenso.com/en/newsroom/news/2020/1/eco-rfid-explained--a-look-behind-the-worlds-greenest-tag#:~:text=The%20sustainable%20ECO%20RFID%20Tag,quality%20while%20being%20cost%20neutral> (accessed on 1 November 2022).
14. Schindler, H.R.; Schmalbein, N.; Steltenkamp, V.; Cave, J.; Wens, B.; Anhalt, A. *SMART TRASH: Study on RFID Tags and the Recycling Industry*; RAND Corporation: Santa Monica, CA, USA, 2012.
15. Kaur, M.E.A. RFID Technology Principles, Advantages, Limitations & Its Application. *J. Comput. Electr. Eng.* **2011**, *3*, 151.
16. McGhee, J.R.; Sinclair, M.; Southee, D.J.; Wijayantha, K.G.U. Strain sensing characteristics of 3D-printed conductive plastics. *Electron. Lett.* **2018**, *54*, 570–572. [[CrossRef](#)]
17. Jamróz, W.; Szafraniec, J.; Kurek, M.; Jachowicz, R. 3D Printing in Pharmaceutical and Medical Applications-Recent Achievements and Challenges. *Pharm. Res.* **2018**, *35*, 176. [[CrossRef](#)] [[PubMed](#)]
18. Bregar, T.; An, D.; Gharavian, S.; Burda, M.; Durazo-Cardenas, I.; Thakur, V.K.; Ayre, D.; Słoma, M.; Hardiman, M.; McCarthy, C.; et al. Carbon nanotube embedded adhesives for real-time monitoring of adhesion failure in high performance adhesively bonded joints. *Sci. Rep.* **2020**, *10*, 16833. [[CrossRef](#)] [[PubMed](#)]
19. Li, D.; Barrington, J.; James, S.; Ayre, D.; Słoma, M.; Lin, M.-F.; Yazdani Nezhad, H. Electromagnetic field controlled domain wall displacement for induced strain tailoring in BaTiO₃-epoxy nanocomposite. *Sci. Rep.* **2022**, *12*, 7504. [[CrossRef](#)] [[PubMed](#)]
20. Doljack, F. PolySwitch PTC Devices-A New Low-Resistance Conductive Polymer-Based PTC Device for Overcurrent Protection. *IEEE Trans. Compon. Hybrids Manuf. Technol.* **1981**, *4*, 372–378. [[CrossRef](#)]